REPORT DOCUMENTATION PAGE

Form Approved
OMB No. 0704-0188

1. REPORT DATE (DD-MM-YYYY)	2. REPORT TYPE	3. DATES COVERED (From - To)
17-10-2007	Final Report	1 Jan 2004 to 31 Dec 2006

4. TITLE AND SUBTITLE
INTEGRATED FLOW CONTROL DEVICES FOR THE DESIGN OF ENHANCED LOW PRESSURE TURBINES

5a. CONTRACT NUMBER

5b. GRANT NUMBER
FA9550-04-1-0024

5c. PROGRAM ELEMENT NUMBER

6. AUTHOR(S)
Jeffrey P. Bons

5d. PROJECT NUMBER

5e. TASK NUMBER

5f. WORK UNIT NUMBER

7. PERFORMING ORGANIZATION NAME(S) AND ADDRESS(ES)
Brigham Young University
Department of Mechanical Engineering
CB 450
Provo, UT 84604

8. PERFORMING ORGANIZATION REPORT NUMBER

9. SPONSORING / MONITORING AGENCY NAME(S) AND ADDRESS(ES)
AFOSR/NA
875 N Randolph St
Arlington VA 22203

10. SPONSOR/MONITOR'S ACRONYM(S)

11. SPONSOR/MONITOR'S REPORT NUMBER(S)

12. DISTRIBUTION / AVAILABILITY STATEMENT
Approved for public release,
distribution unlimited

AFRL-SR-AR-TR-07-0506

13. SUPPLEMENTARY NOTES

14. ABSTRACT
Flow separation limits the efficiency of low-pressure turbines (LPTs) in aircraft engines. Experiments with vortex generator jets (VGJs), conducted in AFRL's low-speed cascade at Wright-Patterson AFB, have demonstrated dramatic reductions in separation losses. The critical science that will enable this design innovation to reach its potential is a comprehensive understanding of the effect of VGJs on a separating boundary layer. Experiments were conducted at BYU to better understand the basic physics of the separation control phenomenon and establish the quantitative links between the underlying flow physics and LPT performance. Understanding gained from these experiments was used to guide the design of a new, high-performance LPT blade at AFRL. The Air Force design codes used to generate the new airfoil included provisions for flow control using vortex generator jets. Experiments with the new profile confirmed the design goal of a 17% increase in blade loading compared to industry standard.

15. SUBJECT TERMS

16. SECURITY CLASSIFICATION OF:			17. LIMITATION OF ABSTRACT	18. NUMBER OF PAGES	19a. NAME OF RESPONSIBLE PERSON
a. REPORT	b. ABSTRACT	c. THIS PAGE		16	19b. TELEPHONE NUMBER (include area code)

2006 Final Report for AFOSR GRANT # FA9550-04-1-0024

Project Title: INTEGRATED FLOW CONTROL DEVICES FOR THE DESIGN OF ENHANCED LOW PRESSURE TURBINES

Principal Investigator: Jeffrey P. Bons, Department of Mechanical Engineering, Brigham Young University, Provo, Utah

Abstract

Flow separation limits the efficiency of low-pressure turbines (LPTs) in aircraft engines. Experiments with vortex generator jets (VGJs), conducted in AFRL's low-speed cascade at Wright-Patterson AFB, have demonstrated dramatic reductions in separation losses. The critical science that will enable this design innovation to reach its potential is a comprehensive understanding of the effect of VGJs on a separating boundary layer. Experiments are underway at BYU to better understand the basic physics of the separation control phenomenon and establish the quantitative links between the underlying flow physics and LPT performance. During the three years of this study, the following tasks were accomplished. Two-component velocity measurements of VGJ evolution were made in a linear cascade for various flow conditions. Data clearly show the presence of streamwise vortices which provide the necessary boundary layer mixing to inhibit separation. A design criterion for the use of steady VGJs is proposed. The effects of elevated freestream turbulence (from 0.3% to 10%) are also addressed in detail. Finally, 3-component PIV measurements of the flowfield with steady and unsteady VGJs highlight major differences between the two control methods. Understanding gained from these experiments was used to guide the design of a new, high-performance LPT blade at AFRL. The Air Force design codes used to generate the new airfoil included provisions for flow control using vortex generator jets. Experiments with the new profile confirmed the design goal of a 17% increase in blade loading compared to industry standard designs. Phase-locked three-component PIV measurements of the suction surface flowfield with unsteady VGJs document the unsteady response of the separation bubble. Time-resolved flow measurements were taken with pulsed VGJs for 2 blade configurations: the Pack B baseline and a new, high-performance design from AFRL (L1M). At low Reynolds number, the L1M has a reattaching separation while the Pack B does not. Measurements indicate that this feature significantly influences the unsteady interaction of the pulsed jet with the separation bubble. Specifically, the non-reattaching bubble has a longer phase lag to recover its fully separated state after being perturbed by the jet. Experiments are underway to assess the impact of upstream wakes on the proposed control methodology.

Full Report

Objectives: Flow separation limits the efficiency of modern low-pressure turbines in aircraft gas turbine engines. Experiments with vortex generator jets, conducted in AFRL's cascade at Wright-Patterson AFB, demonstrated reductions in separation losses at low Reynolds numbers [1]. This was followed by demonstrations of VGJ separation

control at higher Reynolds numbers but with increased blade pitch (ie…fewer blades) [2]. This proof-of-concept demonstrated the potential to design highly-loaded, compact, LPTs with integrated flow control using VGJs. The objective of this research is to understand the fundamental physics of this interaction so that VGJ models can be developed and incorporated into existing LPT design codes. To achieve the required level of flow understanding requires the coupling of experimental, computational, and analytical design studies. As such, detailed flow measurements accomplished at BYU as part of this research are available for code validation elsewhere. The combination of experiment and computation will form the building blocks for understanding the basic physics of the separation control phenomenon, with the results feeding directly into the AFOSR design task of Drs. Rolf Sondergaard and Richard Rivir at AFRL/PRTT.

Approach: Experimental measurements are underway in a modular wind tunnel facility at Brigham Young University. The wind tunnel can be operated in any of four configurations: flat wall no pressure gradient, flat wall with pressure gradient, curved wall no pressure gradient, full LPT cascade with wall curvature and pressure gradient. This sequence allows the independent evaluation of streamwise pressure gradient and wall curvature and their effects on VGJs. A 3-axis traverse system mounted atop the tunnel is used to make two-component velocity measurements using split-film anemometry. Planes of velocity measurements before and after jet injection chart the jet evolution and modifications to the boundary layer. A 3-component PIV system is also employed to allow phase-locked and time-resolved measurements for pulsed jet applications.

Year 1 Progress: During this reporting period, testing has been conducted in the 2-passage Pak-B blade cascade configuration (Figure 1) for 3 blowing ratios ($B = V_{jet}/V_{\infty} = 0, 2, \& 4$) and 4 freestream turbulence levels (0.3%, 3%, 7%, and 10%). The second configuration studied was the flat wall with pressure gradient. A wedge with aft suction (Figure 2) was inserted into a straight wind tunnel test section to provide a streamwise pressure distribution matching that found in the AFRL Pak-B cascade facility. PIV measurements were made in this second configuration for the following conditions: angled steady injection, angled pulsed injection, and normal pulsed injection.

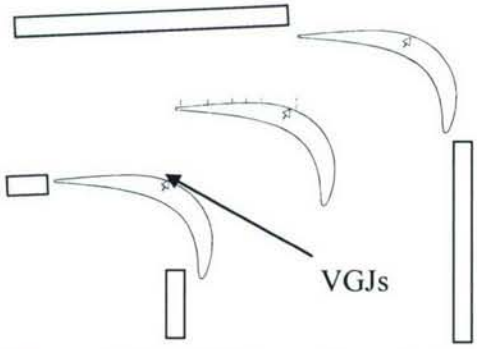

Figure 1: Pak-B Linear Cascade Schematic

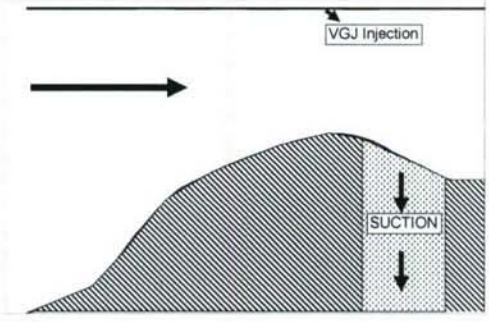

Figure 2: Straight section with Wedge

Results: One of the primary motivations for these experiments is the limited access in the large AFRL cascade facility. This smaller, 2-passage cascade is readily accessed for split-film (2-component) and stereo-PIV (3-component) velocity measurements. The use of a lower blade count cascade was first verified by comparing the pressure (c_p) distribution and blade wake surveys with those presented in [1] (Figures 3 and 4). The results appear to be consistent. [Note: since the VGJ-equipped blade in the 2-passage cascade is the inner blade (see Figure 1), the comparison in Figure 3 uses the pressure surface data from the center blade and the integrated pressure loss surveys in Figure 4 are taken before the blade trailing edge.]

The success of the VGJs in reducing blade separation losses (Figure 4) can be attributed to the creation of streamwise vortices that enhance mixing between the freestream and boundary layer. These are clearly shown using streamwise (u) and wall-normal (v)

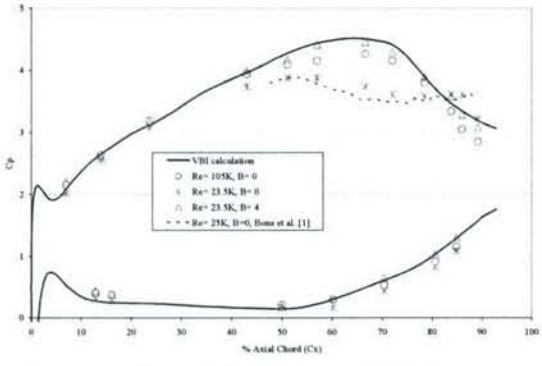

Figure 3: cp distribution for linear cascade

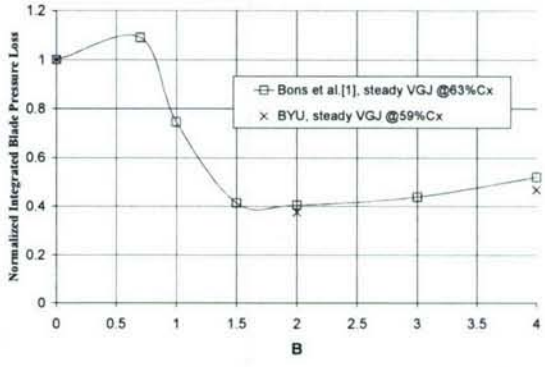

Figure 4: Blade integrated pressure loss

velocity data taken downstream of the jet injection location. Figure 5 shows the v-velocity distribution measured through the vortex centers (at y/D = 3, where D is the jet hole diameter) overlaid on a u-velocity contour plot (normalized by cascade inlet velocity, U_{in}). VGJ injection locations are shown with black arrows and the jet fluid and vortex core are indicated (x is streamwise from jet hole, y is normal, and z is spanwise).

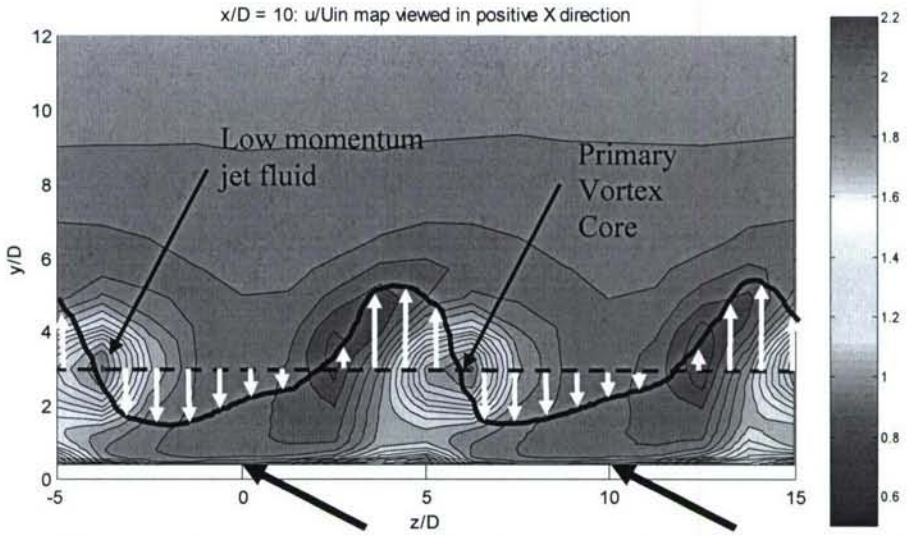

Figure 5: Wall-normal (v) velocity profile taken through vortex centers at y/D = 3 overlaid on streamwise (u) velocity contour map. B = 4, Re = 25k, x/D = 10, 0.3%Tu.

A comparison of the vortex development at two blowing ratio (B = 2 & 4) suggests that separation control is optimized when the jet-induced vortex remains close to the boundary layer. Figures 6a&b compare v-velocity profiles through the vortex centers at two x/D locations downstream of the jets. The more rapid attenuation of the B = 4 v-velocity distribution signals a reduction in vortex strength. Thus, the greater massflow penalizes the vortex development and causes a slight reduction in effectiveness (Figure 4). A VGJ effectiveness parameter can be formed by the ratio of the convective timescales for the jet to traverse the boundary layer (δ/U_{jet}) and the freestream to traverse the jet hole (D/U_e). This new parameter ($\tau_{VGJ} = \delta$ /DB) can be optimized for a given application of steady VGJs. Values of $\tau_{VGJ} \cong 1$ appear to be optimum for this configuration.

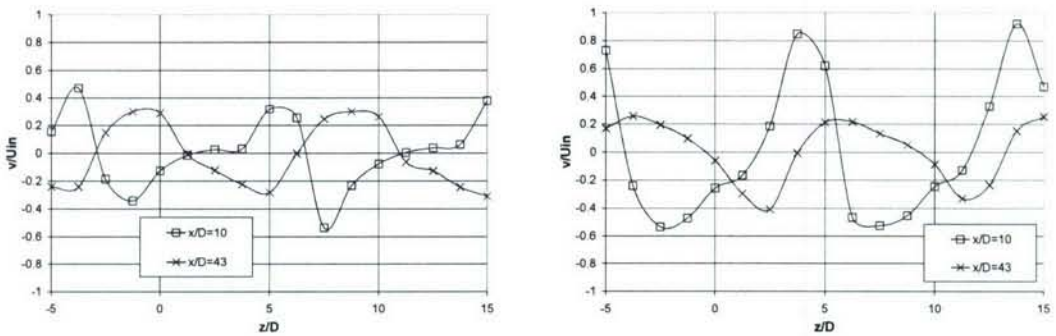

(a) v/U_{in}, B = 2 **(b) v/U_{in}, B = 4**

Figures 6a&b: Profiles of wall normal velocity at x/D = 10 and 43. Re = 25k. Data is taken at constant y/D through the vortex centers.

In practice, LPTs have elevated freestream turbulence levels ($Tu = u_{rms}/U$). Thus, four levels of Tu were studied to understand the influence of elevated turbulence on steady

VGJ effectiveness. Figure 7 shows u/Uin contour plots at the furthest downstream location (x/D ≅ 42) for B = 2 with the four different cascade inlet turbulence levels (Tu_{in}). Increasing levels of freestream turbulence result in a more rapid dissipation of the VGJs and limit their effectiveness. At the two highest levels of turbulence, the boundary layer separation is completely eliminated (without blowing); thus, the larger freestream velocity levels shown in the contour plots. At elevated Tu levels, jet blowing above B = 2 reduces effectiveness and incurs a larger penalty to the gas turbine cycle due to the higher massflow requirements.

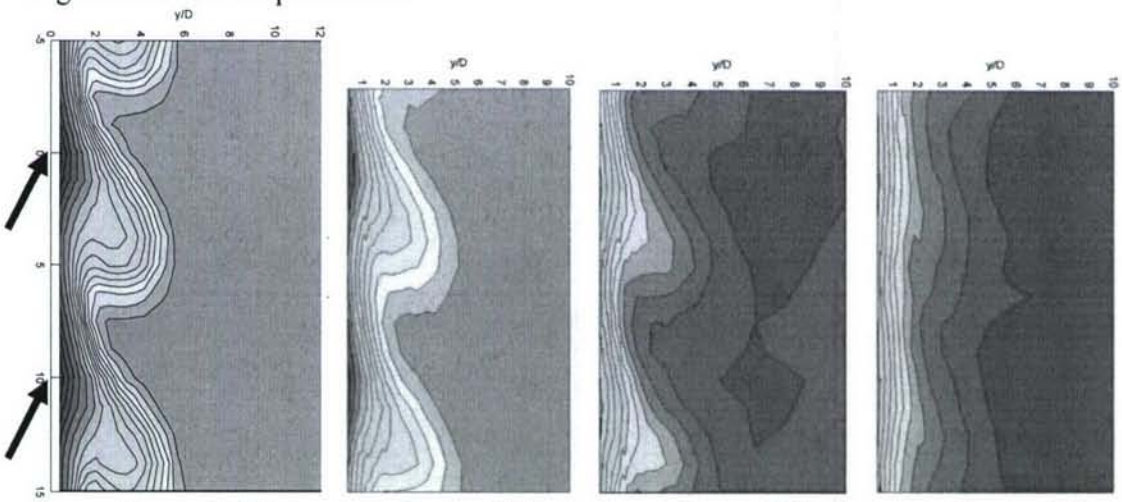

Tu_{in} = 0.3% **Tu_{in} = 3%** **Tu_{in} = 7%** **Tu_{in} = 10%**

Figure 7: Contour plots of streamwise (u/U_{in}) velocity at x/D = 42 for 4 levels of Tu_{in}: 0.3%, 3%, 7%, and 10%. Colorbar is identical to that shown in Figure 5. Re = 25k.

Successive planes of 3-component PIV data were processed to produce streamwise vorticity contours for steady VGJ injection into a straight tunnel (with no streamwise pressure gradient). Figures 8a&b show differences in vortex development for the case of normal injection vs. the skewed VGJ injection (with 30° pitch and 90° skew angles).

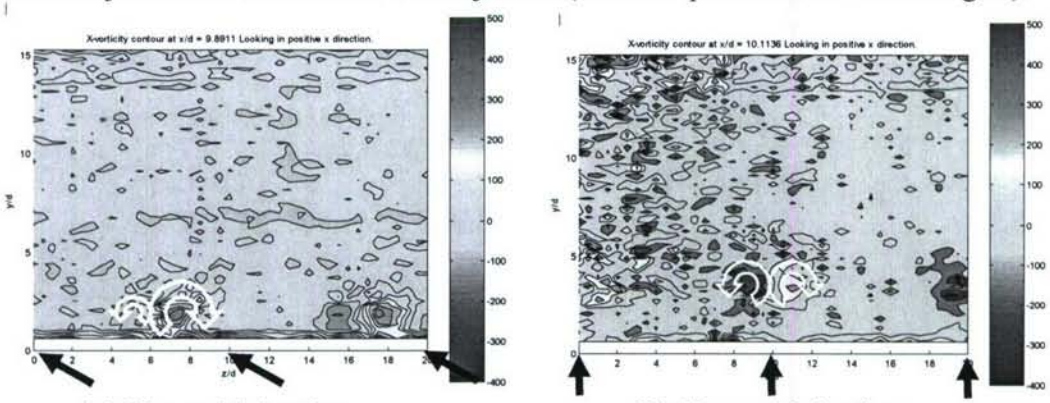

(a) Skewed injection **(b) Normal injection**

Figure 8: Contour maps of streamwise vorticity at x/D = 10 for (a) skewed and (b) normal jet injection into a constant velocity freestream with laminar boundary layer (Tu = 0.3%).

The stronger vortices generated by the skewed injection remain closer to the wall and produce the desired freestream entrainment into the boundary layer. They also produce a roll-up of boundary layer fluid away from the wall as shown with pulsed jet data in Figure 9. Even well after the jet fluid has been convected beyond the measurement domain (Figure 9b), the roll-up of the boundary layer due to the vortex motion is still evident.

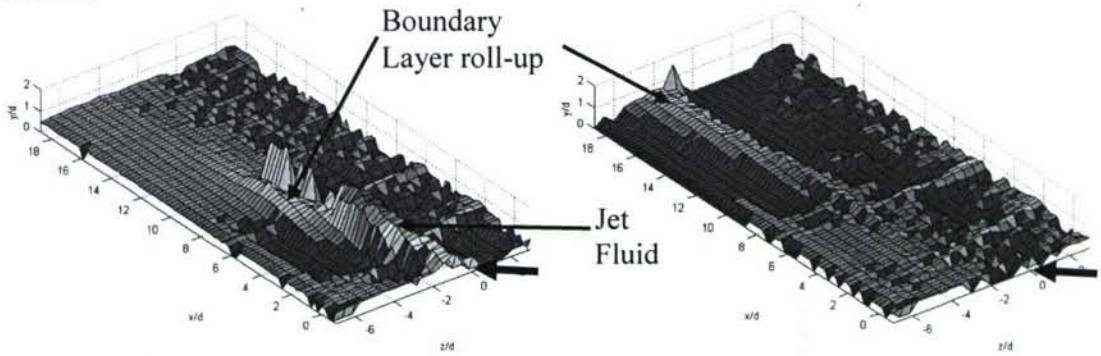

(a) jet ON - 15% of pulsing cycle **(b) jet OFF - 80% of pulsing cycle**

Figure 9: Surface maps of $u/U_{in} = 0.5$ for pulsed VGJ injection into a constant U_∞ laminar boundary layer (Tu = 0.3%). $B_{max} \cong 2$ with frequency of 5Hz at 25% duty cycle.

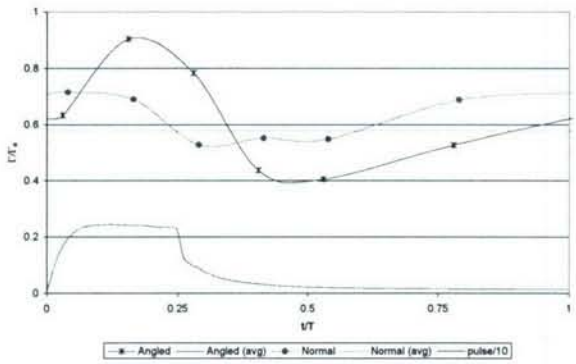

Figure 10: Integrated loss coefficient vs. pulse phase. Data taken at x/D = 20 with wedge configuration. Normal vs. pulsed injection.

PIV measurements were also taken with the pulsed jets in the wedge configuration. Testing was conducted for both normal and skewed jet injection at the same pulsing frequency and duty cycle. Results showed greater range of control using the skewed jet injection, though the cycle-averaged separation losses were comparable for the two configurations. Figure 10 shows the integrated downstream losses as a function of pulsing phase. Specific flow features noted in phase-locked velocity maps suggest subtle differences in the two control methods.

Year 2 Progress: During this reporting period, a new low-pressure turbine blade was designed by Drs. John Clark and Pete Koch at AFRL/PRTT using AFRL design codes with integrated VGJs. The baseline for the design was the Pratt-Whitney low Mach number Pack B profile. Using this as a point of departure, the blade pitch was increased with constant blade metal angles until the Zweifel coefficient of 1.34 was achieved (17% higher than the Pack B). The results of Praisner et al. [3] suggested that aft-loaded airfoils were prone to more severe lapses in efficiency with decreasing Reynolds number than front-loaded airfoils at the same turning. Accordingly, the new airfoil shape (here denoted as "L1M") was modified via the available airfoil design parameters until a "balanced" loading was achieved. The new airfoil has a point of minimum pressure that occurs on the suction side of the airfoil at approximately 47% axial chord, whereas maximum velocity occurs at roughly 65% c_x for the Pack B. The new blade has a reduced solidity (0.99 vs. 1.13) as shown in Fig. 11. The placement of the VGJ holes was guided by previous work by Sondergaard, Rivir, and Bons [1,2]. They were located at 50% c_x, just downstream of the minimum pressure and just upstream of the predicted separation location using the MISES code.

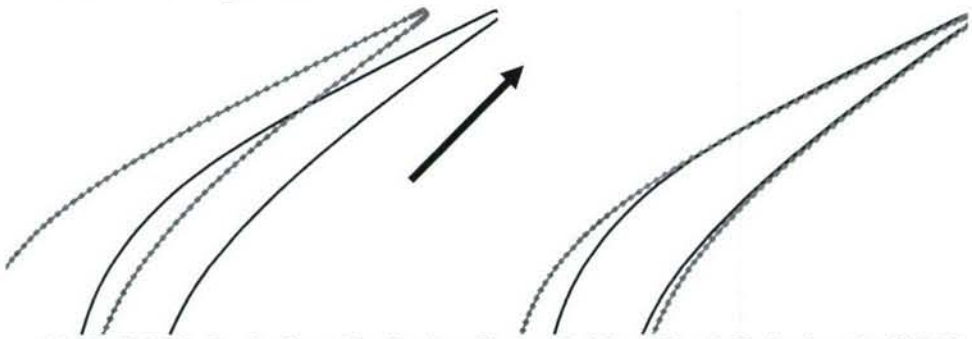

Figure 11: L1M blade design (dashed red) overlaid on Pack B design (solid black). Aft portion of cascade only.

A 3-blade linear cascade was fabricated at BYU using the new L1M design. Blade surface pressure measurements taken at Re = 20,000 and 50,000 confirmed the design objectives of a more stable, higher-performance LPT blade (Fig. 12). As shown in the figure, the region of separation for the uncontrolled (B = 0, where B is the jet blowing ratio) closely follows the MISES prediction for Re=50,000. At the lower Reynolds number (20,000), the predicted separation zone is longer than that shown in the data, nevertheless both the prediction and the data show boundary layer reattachment. This result is different than the Pack B behavior at low Reynolds number, where the separation does not reattach to the blade resulting in a large wake loss profile. The improved performance is due to the more forward-loaded blade design. Because the uncontrolled performance of the L1M was so favorable, the need for flow control with this new design was limited. The application of steady jet blowing (B=2) was successful in eliminating the separation zone as shown in Fig. 12, however the anticipated improvement in blade losses with flow control was not realized since the uncontrolled separation bubble is closed.

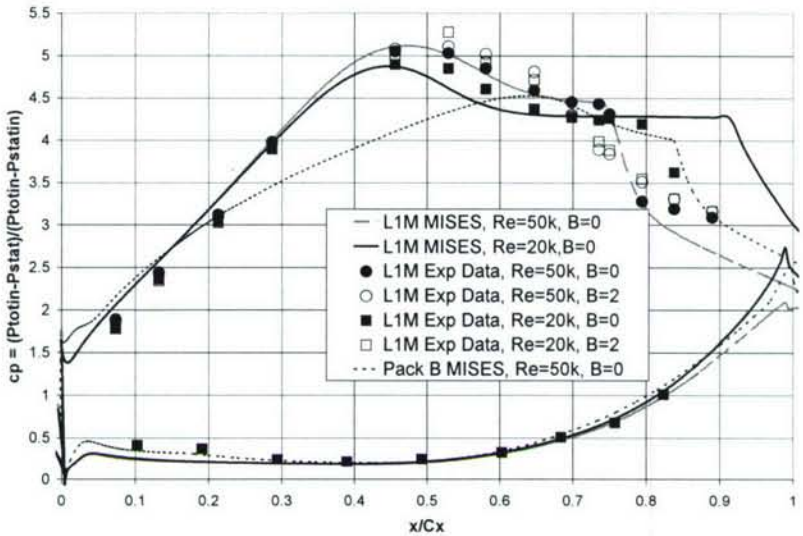

Figure 12: Experimental L1M c_p distribution for Re = 20,000 & 50,000 compared to MISES prediction. (Experimental data for B = 0 & 2) Pack B MISES calculation at Re = 50,000 shown for comparison.

Based on these results and observations, some important conclusions can be drawn regarding low pressure turbine blade design. First, the design space for high lift airfoils appears to be larger than previously thought. Furthermore, this design was achieved without serious loss increases at low Re by avoiding aft-loading of the blade profile. The fact that these performance improvements were accomplished without relying on flow control leads to a second important conclusion. Flow control concepts must be integrated into the design process up front. That is, the most pragmatic approach to solving a Reynolds-lapse problem might be aerodynamic redesign, provided that one can adequately predict boundary layer behavior. A flow control fix is likely the last resort. However, if one can determine the true limits on design loading within the expanded design space defined by the new modeling capability, then flow control could be used to push loading to hitherto unachievable levels. This is to be the subject of a future study.

Detailed three-component PIV measurements of the L1M separation bubble and its interaction with pulsed VGJs were taken to provide previously unavailable spatial resolution and clarity of the fluid mechanics of separation control. The LaVision 3-component stereo PIV system was mounted on a 3-axis traverse located below the transparent acrylic cascade section to enable a full mapping of the flow field. Two overlapping data collection window positions (Fig. 13) were used to encompass the region occupied by the L1M separation bubble. To collect the data, the laser sheet was oriented in the x-y plane. Forty separate images at each z location were recorded, processed, and averaged. This procedure was repeated at increments of 1mm in z in order to generate a three-dimensional block of velocity data across the 23mm hole pitch (i.e. 24 individual z elevations).

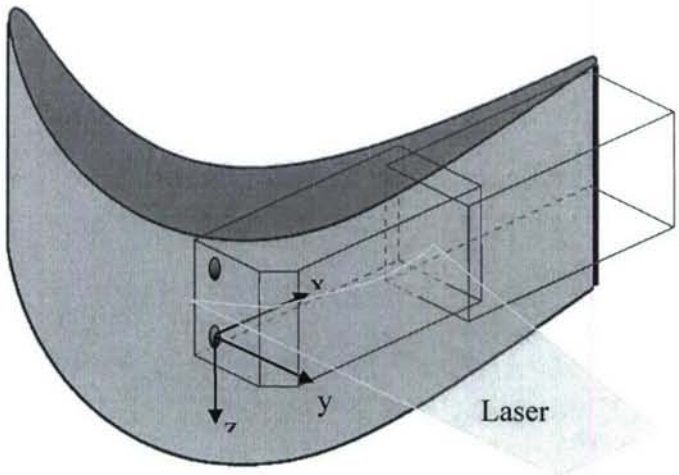

Figure 13: Schematic of PIV data collection regions relative to test blade.

PIV data taken without flow control show excellent agreement with the separation, reattachment, and boundary layer transition locations predicted by the AFRL design code. This favorable result is due in large part to the updated transition model developed by Praisner and Clark [4]. Based on previous success with the application of pulsed VGJs [1], the jets were actuated at 5Hz with a duty cycle of 25% to observe the interaction of the separation bubble with the unsteady jet pulse. Data were acquired at 8 points in the jet period as shown in Fig. 14 overlaid on the jet hole exit blowing ratio time history. The results are best displayed using three-dimensional surface plots of the u/U_{in}=0.75 surface (Fig. 15). Due to the factor of two acceleration in the blade passage (from U_{in} to U_{ex}), this surface is in the lower part of the boundary layer and clearly identifies the zone of separated flow. The freestream flow enters from the bottom right corner and jet injection is in the negative z direction also from the lower right corner of the plot (Fig. 13 shows the flow domain).

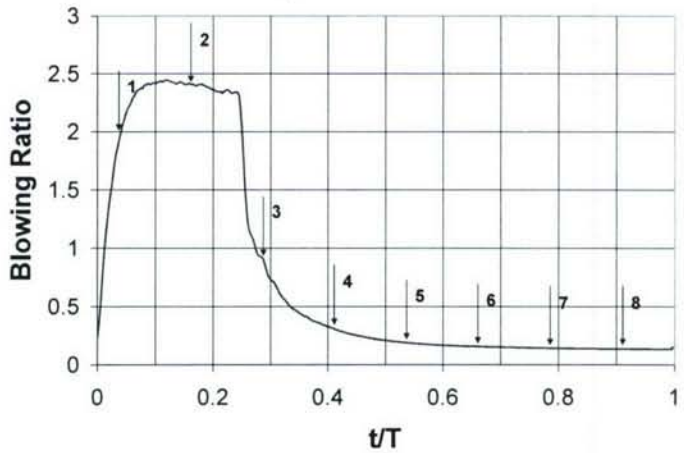

Figure 14: Jet hole exit blowing ratio time history (B vs. t/T) for pulsed VGJ operation at 5Hz and 25% duty cycle. Arrows indicate PIV data collection points.

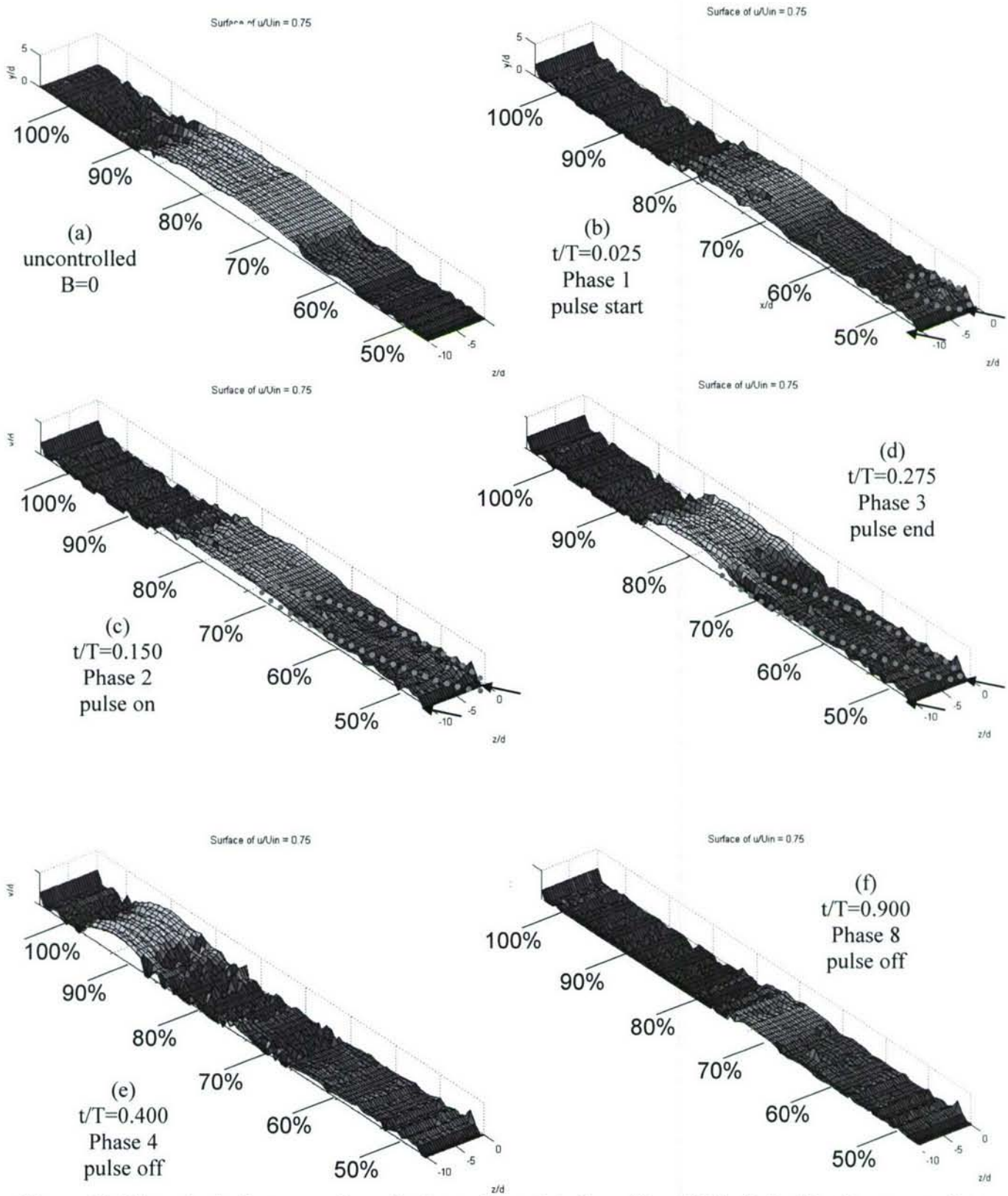

Figure 15: Phase-locked streamwise velocity surface plots for $u/U_{in} = 0.75$. Pulsed jet flow control at Re=20k. Black arrows indicate jet flow and red ovals represent jet fluid.

Figure 15a shows the uncontrolled extent of the separation zone, while the remaining 5 plots are from different points in the jet pulse as shown in Fig. 14. The red dashed ovals in plots Phases 1-3 identify the jet trajectory which impinges on the leading edge of the separation bubble before it has grown to its full, uncontrolled size. Subsequently, the bubble is squeezed off the end of the blade by flow reattachment, becoming more condensed as it moves downstream. Phases 5-7 (not shown) exhibit essentially fully attached flow until the separation bubble resurfaces near 70% c_x in Phase 8. These flow dynamics are markedly different from previous measurements of the Pack B separation bubble [1] and are currently being explored in greater detail.

Year 3 Progress: During the last reporting period, a new low-pressure turbine blade (L1M) was designed by Drs. John Clark and Pete Koch at AFRL/PRTT using AFRL design codes with integrated VGJs. The L1M has 17% Zweifel loading coefficient compared to the baseline Pack B profile. The new blade has a reduced solidity (0.99 vs. 1.13) as shown in Fig. 11.

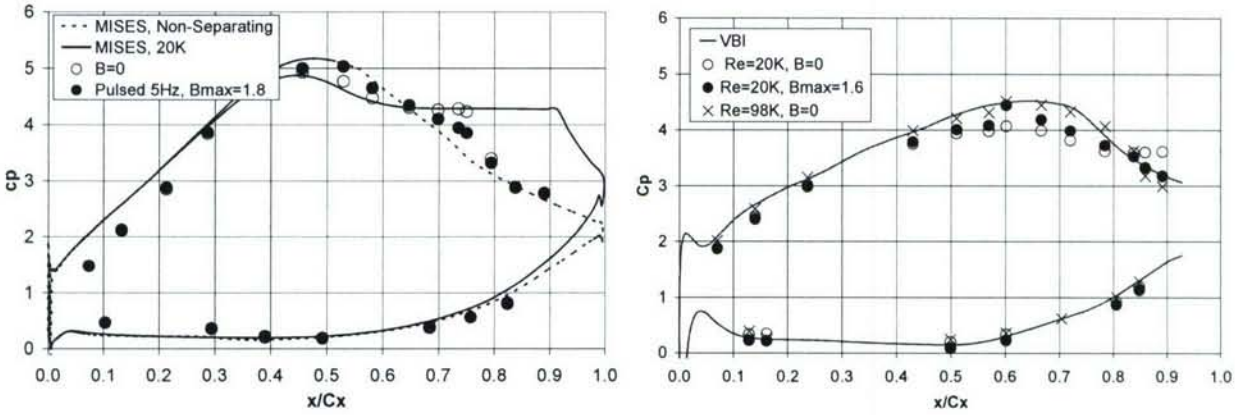

a) L1M **b) Pack B**

Figure 16: c_p distributions for (a) L1M at B=0 and B_{max}=1.8 (5Hz) at Re_c=20,000 vs. MISES prediction (b) Pack B at B=0 and B_{max}=1.6 (5Hz) at Re_c=20,000 & B=0 at Re_c = 90,000 vs. VBI prediction.

A side-by-side comparison of the performance of these two designs is shown in Fig. 16. The L1M has a peak c_p at approximately 47% axial chord (c_x), compared to roughly 65% c_x for the Pack B. Figure 16 includes data with pulsed VGJ blowing with the jet holes located at 50% c_x on the L1M and 59% c_x on the Pack B (near the minimum pressure in both cases). In both cases, pulsed jet actuation eliminates the separation bubble noted in the time-averaged static pressure distribution. Time-resolved measurements were made of both flowfields using a single-component hot-film sensor traversed in a plane perpendicular to the blade span. Figure 17 displays a series of mean velocity contours at different phases during the 200ms pulsing period. The full period was divided into 24 phases, with the jet active during phases 1-6 (25% duty cycle).

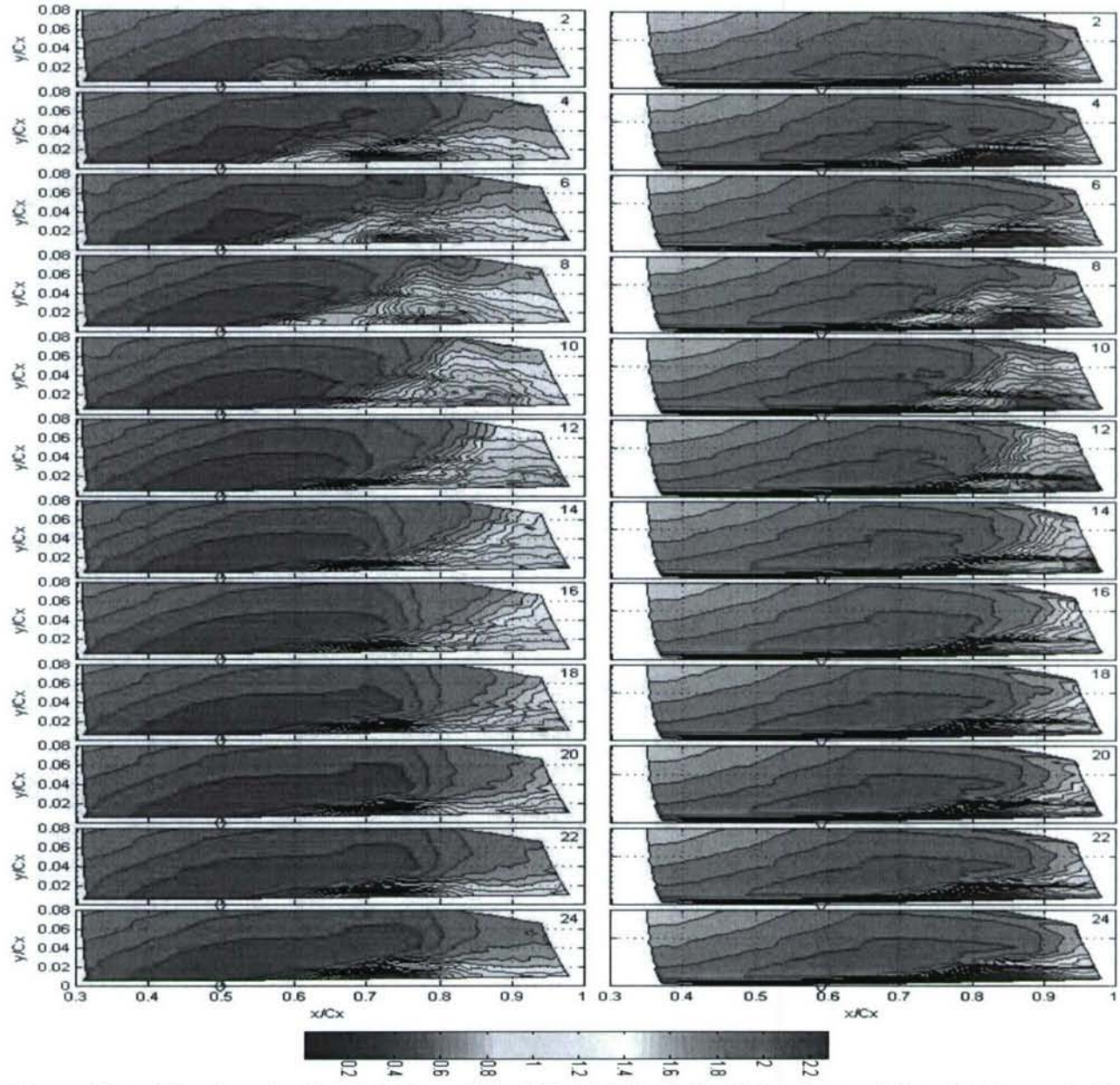

Figure 17: $\tilde{u}$ /U_{in} plots for L1M (left) and Pack B (right). Pulsed blowing at 5Hz with $B_{max} \cong 2$. Phase number indicated in upper right corner.

Figure 17 is displayed in axial chord coordinates with the flow from left to right and the VGJ injection location indicated with a diamond symbol near the bottom of each figure (y=0 is the suction surface of the blade). Essentially the jet disturbance causes the separation bubble (the region of blue, low momentum fluid) to bunch up and eventually be swept off the trailing edge of the blade. Phase-locked intermittency measurements indicate that the jet does this by promoting early boundary layer transition. Time-history plots of flow unsteadiness and intermittency at a fixed wall distance of y = 3% c_x show the trajectory of the jet disturbance and the relaxation of the boundary layer fluid following the passing of the jet fluid (Fig. 18). A "calmed" region of relatively quiet

fluid appears at the furthest downstream excursion of the boundary layer transition line (indicated by red oval in Fig. 18).

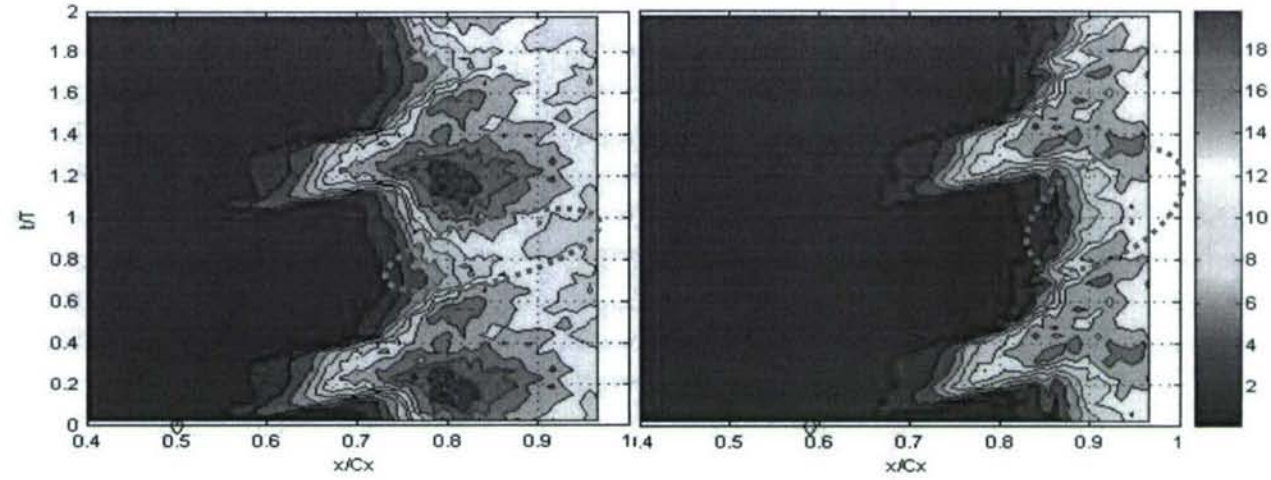

L1M – u_{rms}/U_{in} [%] at y/c_x =0.033 **Pack B – u_{rms}/U_{in} [%] at y/c_x =0.036**

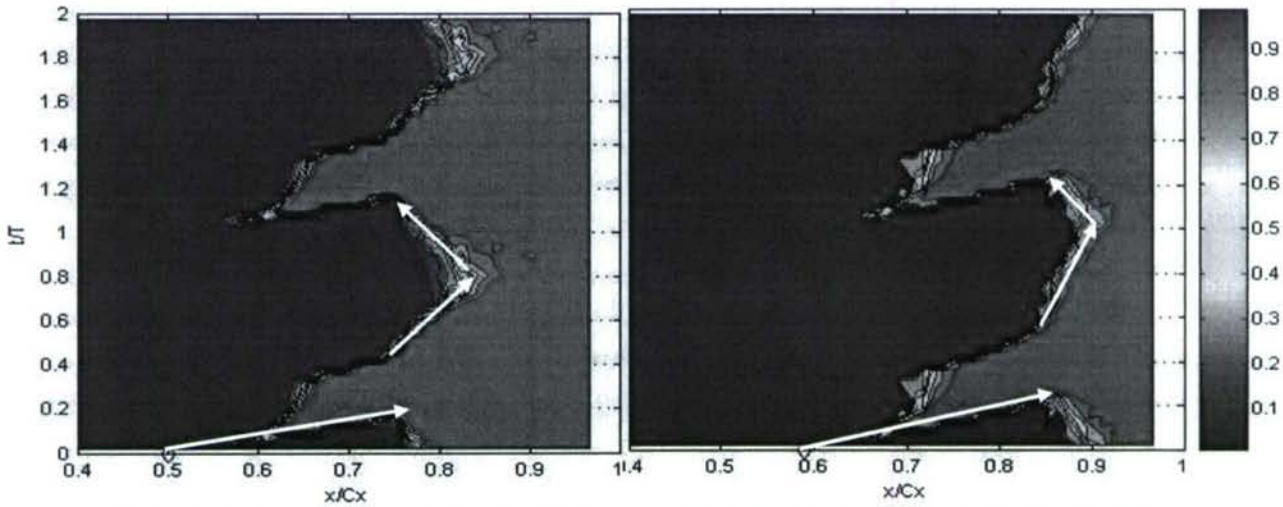

L1M – intermittency at y/c_x =0.033 **Pack B – intermittency at y/c_x =0.036**

Figure 18: u_{rms}/U_{in} and intermittency time-space plots for L1M and Pack B.

The mean velocity data in Fig. 17 was interrogated to determine the separation bubble size and upstream and downstream extent as a function of phase during the jet pulsing period. The results show that the closed separation bubble on the L1M blade responds more rapidly to the jet injection than the non-reattaching Pack B separation. The L1M also returns to its separated state more rapidly as shown in Fig. 19 (b). The Pack B remains at its minimum separation size (30% of the uncontrolled bubble size) from phases 16-23 when the jet disturbance has already been convected off the end of the blade. Apparently, the large amplitude flow oscillations associated with the ejection of a non-reattaching separation bubble create a temporary flow inertia that maintains the attached state for some finite period of time (50ms in this case) after the separation has been eliminated and the control is off.

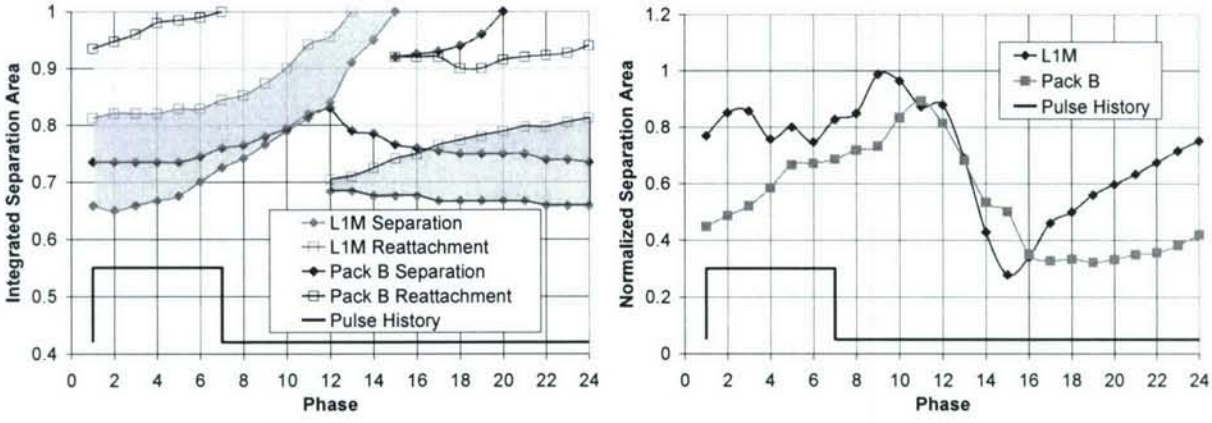

(a) (b)

Figure 19: Separation bubble evolution vs. pulsing phase for L1M and Pack B: a) separation bubble maximum upstream and downstream extent and b) integrated separation bubble area normalized by bubble size with no control (B = 0).

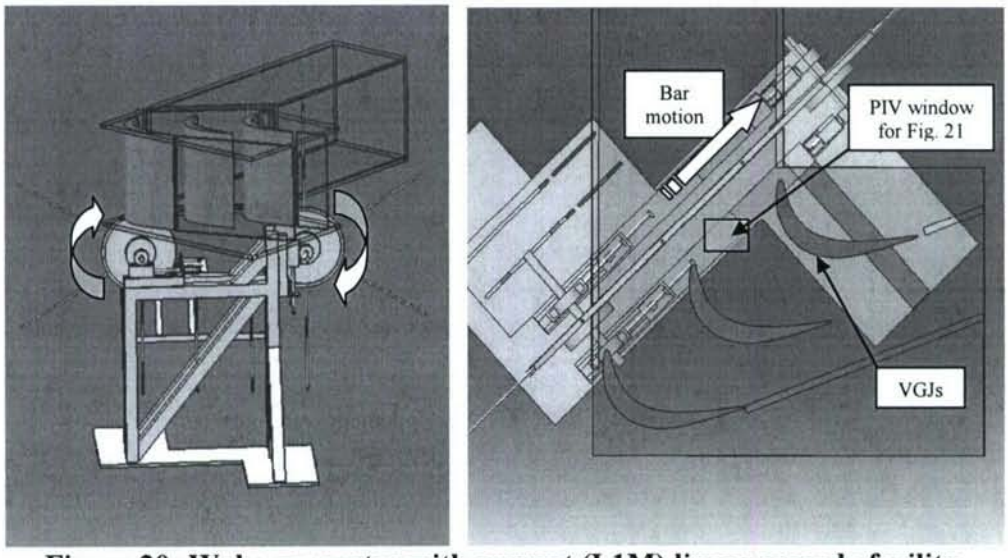

Figure 20: Wake generator with current (L1M) linear cascade facility.

A wake generator was designed and constructed during the past year to allow simulation of moving upstream blade rows in the linear cascade facility (Fig. 20). PIV measurements taken near the cascade inlet plane (see window in Fig. 20) show the low momentum fluid associated with the convected wake disturbance at three distinct times relative to the wake passing (Fig. 21). This facility is being used to examine the possible synchronization of VGJ pulsing with the wake passing frequency.

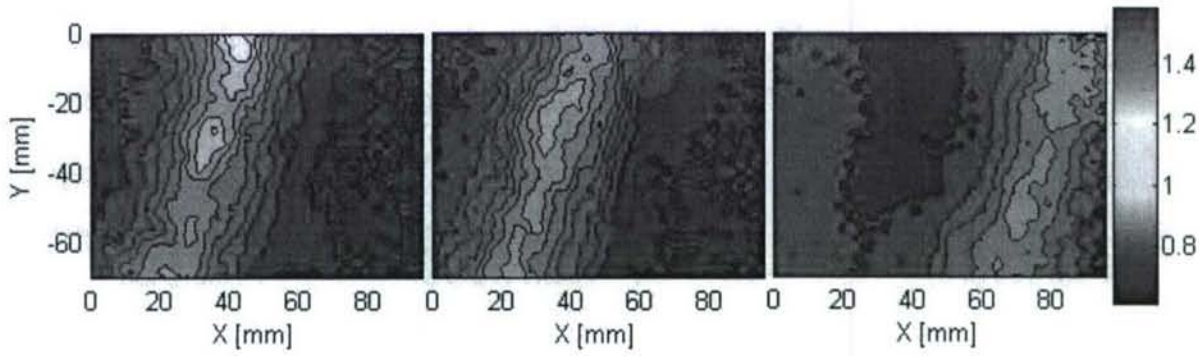

Figure 21: PIV velocity data showing 3 successive bar passing phases at cascade inlet.

Acknowledgement/Disclaimer

This work was sponsored (in part) by the Air Force Office of Scientific Research, USAF, under grant/contract number FA9550-04-1-0024. The views and conclusions contained herein are those of the author and should not be interpreted as necessarily representing the official policies or endorsements, either expressed or implied, of the Air Force Office of Scientific Research or the U.S. Government.

References

1. Bons, J., Sondergaard, R., and Rivir, R., 2001, "Turbine Separation Control Using Pulsed Vortex Generator Jets", *ASME J of Turbomachinery*, Apr 2001, pp. 198-206.
2. Sondergaard, R., Bons, J., Sucher, M., and Rivir, R., 2002, "Reducing LPT Stage Blade Count Using VGJ Separation Control," ASME Paper No. GT-2002-30602.
3. Praisner, T. J., Grover, E. A., Rice, M. J., and Clark, J. P., 2004, "Predicting Transition in Turbomachinery, Part 2- Model Validation and Benchmarking," ASME Paper No. GT-2004-54109.
4. Praisner, T. J. and Clark, J. P., 2004, "Predicting Transition in Turbomachinery, Part 1- A Review and New Model Development," ASME Paper No. GT-2004-54108.

Personnel Supported During Duration of Grant

Laura Hansen, Rich Eldredge, Dan Reimann, Matt Bloxham Graduate Students, BYU
Jeffrey Bons Associate Professor, Brigham Young University

AFRL Points of Contact

Rolf Sondergaard, Richard Rivir, John Clark, and Peter Koch, AFRL/PRTT, WPAFB.

Publications

1. "Influence of Vortex Generator Jet-Induced Transition on Separating Low Pressure Turbine Boundary Layers," by D. Reimann, M. Bloxham, K.L. Crapo, J.D. Pluim, and J.P. Bons. Presented at the 3rd AIAA Flow Control Conference in San Francisco, 5-8 June, 2006 (paper #AIAA 2006-2852). Submitted for publication in *AIAA Journal of Propulsion and Power*.
2. "The Effect of VGJ Pulsing Frequency on Separation Bubble Dynamics," by M. Bloxham, D. Reimann, and J. P. Bons. Presented at the AIAA 44th Aerospace

Sciences Meeting and Exhibit in Reno, NV, 9-12 Jan 2006 (paper #AIAA 2006-0876).

3. "Separated Flow Transition on an LP Turbine Blade with Pulsed Flow Control," by J.P. Bons, D. Reimann, and M. Bloxham. Presented at the 2006 IGTI conference in Barcelona, 8-11 May, 2006. Paper #GT2006-90754.. Accepted for publication in *ASME Journal of Turbomachinery*.
4. "Phase-Locked Flow Measurements of Pulsed Vortex-Generator Jets in a Separating Boundary Layer," by L. Hansen and J.P. Bons. *AIAA J. Propulsion and Power,* Vol. 22, No 3, May-June 2006, pp. 558-566.
5. "Detailed Measurements of Vortices Generated Using Steady VGJs for Separation Control," by Eldredge, R. and Bons, J.P.. Submitted to *AIAA J. Propulsion and Power*. Manuscript currently in review.
6. "Time-Resolved Flow Measurements of Pulsed Vortex-Generator Jets in a Separating Boundary Layer," by L. Hansen and J.P. Bons. Presented at the 2nd AIAA Flow Control Conference in Portland, OR, 28 June – 1 July (paper #AIAA 2004-2203).
7. "Active Control Of A Separating Boundary Layer With Steady Vortex Generating Jets - Detailed Flow Measurements," by R. Eldredge and J.P. Bons. Presented at the AIAA 42nd Aerospace Sciences Meeting and Exhibit in Reno, NV, 5-8 Jan 2004 (paper #AIAA 2004-0751).
8. "Phase-Locked Flow Measurements of Pulsed Vortex-Generator Jets in a Separating Boundary Layer," by L. Hansen and J.P. Bons. Submitted to *AIAA J. Propulsion and Power*. Manuscript currently in review.
9. "Designing Low-Pressure Turbine Blades with Integrated Flow Control," by J.P. Bons, L.C. Hansen, J.P. Clark, P.J. Koch, and R. Sondergaard. Presented at IGTI 2005 in Reno, NV, June 2005. Paper # GT2005-68962.
10. "The Effect of Elevated Freestream Turbulence on Separation Control with Vortex-Generating Jets," by D.H. Olson, D. Reimann, M. Bloxham, and J.P. Bons. Presented at the AIAA 43rd Aerospace Sciences Meeting and Exhibit in Reno, NV, 10-13 Jan 2005 (paper #AIAA 2005-1114).